PHOBOS Beam Use Proposal for RHIC Runs V–VIII

The PHOBOS Collaboration

B.B.Back[1], M.D.Baker[2], M.Ballintijn[4], D.S.Barton[2], R.R.Betts[6], A.A.Bickley[7], R.Bindel[7], W.Busza[4], A.Carroll[2], Z.Chai[2], M.P.Decowski[4], E.García[6], T.Gburek[3], N.George[2], K.Gulbrandsen[4], C.Halliwell[6], J.Hamblen[8], M.Hauer[2], C.Henderson[4], D.J.Hofman[6], R.S.Hollis[6], R.Hołyński[3], B.Holzman[2], A.Iordanova[6], E.Johnson[8], J.L.Kane[4], N.Khan[8], P.Kulinich[4], C.M.Kuo[5], W.T.Lin[5], S.Manly[8], A.C.Mignerey[7], R.Nouicer[2,6], A.Olszewski[3], R.Pak[2], C.Reed[4], C.Roland[4], G.Roland[4], J.Sagerer[6], H.Seals[2], I.Sedykh[2], C.E.Smith[6], M.A.Stankiewicz[2], P.Steinberg[2], G.S.F.Stephans[4], A.Sukhanov[2], M.B.Tonjes[7], A.Trzupek[3], C.Vale[4], G.J.van Nieuwenhuizen[4], S.S.Vaurynovich[4], R.Verdier[4], G.I.Veres[4], E.Wenger[4], F.L.H.Wolfs[8], B.Wosiek[3], K.Woźniak[3], B.Wysłouch[4]

[1] Argonne National Laboratory, Argonne, IL 60439-4843, USA
[2] Brookhaven National Laboratory, Upton, NY 11973-5000, USA
[3] Institute of Nuclear Physics PAN, Kraków, Poland
[4] Massachusetts Institute of Technology, Cambridge, MA 02139-4307, USA
[5] National Central University, Chung-Li, Taiwan
[6] University of Illinois at Chicago, Chicago, IL 60607-7059, USA
[7] University of Maryland, College Park, MD 20742, USA
[8] University of Rochester, Rochester, NY 14627, USA

July 30, 2004

Over the last four years, the RHIC complex, and PHOBOS in particular, have provided a rich and varied systematic dataset of Au+Au, d+Au and p+p collisions. These data span a collision energy range from $\sqrt{s_{NN}} = 19.6$ to 200 GeV, a pseudorapidity range from $-5.4 < \eta < +5.4$ and a centrality range from 2–360 participating nucleons ($\langle N_{part} \rangle$). Based on this dataset, a consensus is building that a qualitatively new form of matter has been seen at RHIC (and perhaps at lower energies as well). In particular, we have seen evidence for a strongly interacting medium with extremely high energy density, whose description in terms of hadronic degrees of freedom is inappropriate [1].

It is our view that the best strategy for further characterizing this matter is to study it systematically as a function of energy and beam species. So far, each new energy and species run has led to surprises and qualitatively new results. The latest results from the 200 GeV d+Au (Run III) and 62.4 GeV Au+Au (Run IV) datasets are no exception, as detailed below. There is every reason to believe that a continued push for variety in the form of lighter ion collisions will lead to new discoveries. Furthermore, even in the absence of major surprises, such data will provide a critical test of how the new form of matter "[responds] to variations in the initial conditions" and will allow for "extended jet studies" as described in the December 2003 report of the BNL PAC [2] under the heading of "Key Physics Questions for Future Heavy Ion Research".

The PHOBOS detector provides unique capabilities at RHIC with a demonstrated ability to measure total charge multiplicity, $dN/d\eta$, and elliptic and directed flow over eleven units of pseudorapidity as well as spectra down to transverse momenta of 0.03 GeV/c.

Additionally, having almost complete acceptance for charged particles led to the ability to make precision centrality bins in small systems (such as d+Au). In particular, the large particle acceptance minimizes the centrality smearing caused by Poisson fluctuations and also allows us to test for and remove multiplicity biases which might occur when you measure yields and "centrality" in the same detector.

We propose that the coming runs at RHIC be dedicated to providing as broad a variety of collision species and energies as possible in order to exploit the unique features of PHOBOS in a timely fashion before the experiment ends and these capabilities are lost, or at least diminished, at RHIC. In particular, we consider a very light ion species, such as Si+Si, the highest priority because it enables the largest contrast with Au+Au and because an extensive world dataset of lower energy S+S, Si+Si and Si+Al collisions exists to help contextualize any new results (see Refs. [3–15] for a partial listing).

1. Progress During the Past Year

The past year has been successful both scientifically and technically for PHOBOS (and RHIC). On the scientific front, the PHOBOS collaboration submitted eight new papers to refereed journals [16–23]. On the technical front, the RHIC accelerator was very successful. They were able to provide higher than expected luminosity, higher than expected uptimes and shorter than expected setup times for changing beam energy. Furthermore, the detectors, including PHOBOS, were able to exploit the surprisingly high luminosities despite the triggering and datataking challenges they represented. Finally lab management and the U.S. D.O.E. capitalized on these successes by extending the running time in order to allow a 62.4 GeV Au+Au run. Taken together, these successes led to substantial progress being made on the PHOBOS multi-year Beam Use Proposal (BUP) from last year. The remainder of this section will outline some of the scientific highlights from the last year as well as the progress made on last years BUP.

1.1. Further results from d+Au

At the time of the last beam use proposal, the four RHIC collaborations had just submitted the first results from the critical d+Au "control experiment" [24–27], showing that high p_T particle production is not suppressed from the expected N_{coll} scaling near midrapidity. One concern, particularly for PHOBOS, was the fact that our result for R_{dAu} for $0.2 < \eta < 1.4$ was slightly lower and, in fact, barely consistent with the results of the other three experiments, all of which were making measurements nearer to midrapidity. Was this due to an unexpectedly strong pseudorapidity dependence or was it a genuine experimental discrepancy?

Since then, BRAHMS [28] and PHOBOS (see Figure 1) [21] have published clear evidence of a strong pseudorapidity dependence in R_{dAu} at moderate p_T, with the BRAHMS result extending to $\eta = 3.2$. Furthermore, PHENIX has shown evidence that this eta dependence yields a large enhancement for $\eta \sim -2$ (i.e. in the Au-going direction) [29]. While there are qualitative explanations of the forward-rapidity suppression in terms of parton saturation models [30], this overall phenomenon is still not fully understood, particularly in the backward (Au-going) hemisphere [31].

Another unexplained phenomenon in $d + Au$ is the surprising lack of centrality dependence in the $\bar{\text{p}}$/p ratio seen in Figure 2. The naïve expectation, supported by the

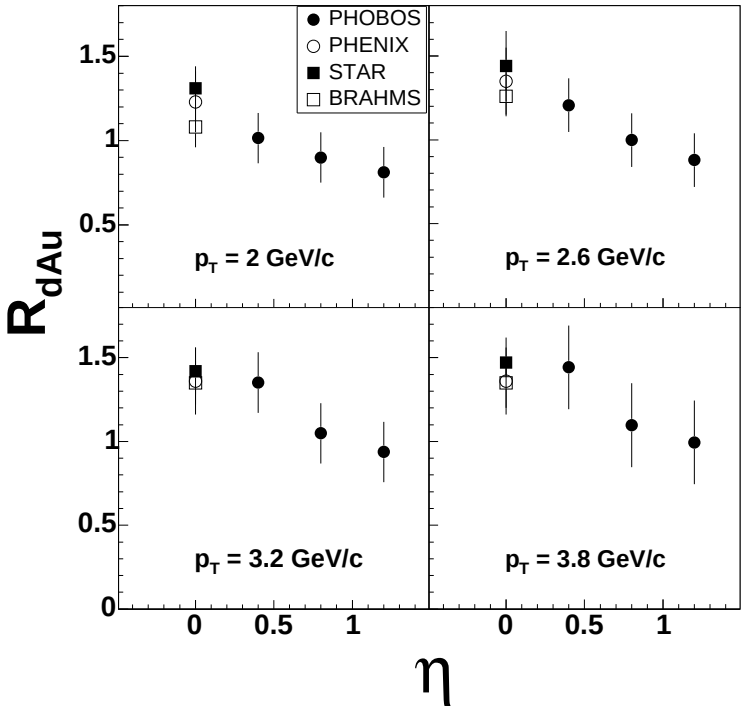

Figure 1. Nuclear modification factor R_{dAu} for four different values of p_T for three different η bins. The error bars show the systematic uncertainty (90% C.L.) of the fitted data points. PHENIX, STAR, and BRAHMS points are from Refs. [25–27]. Figure taken from Ref. [21].

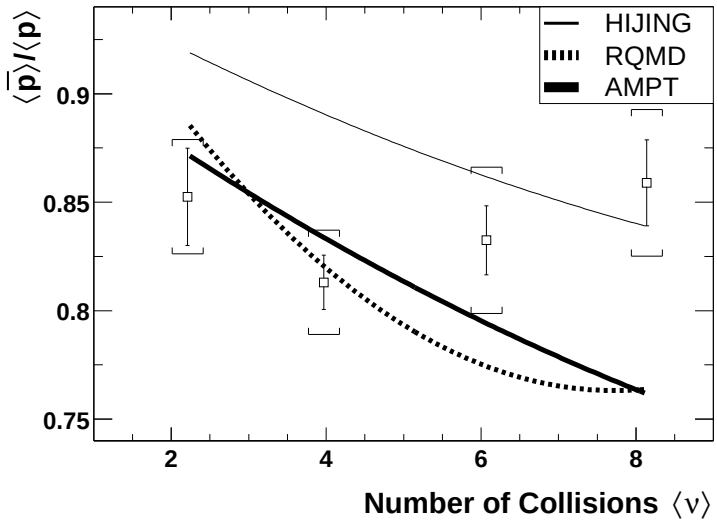

Figure 2. Antiproton to proton ratio compared with models. The squares are the d+Au data at $\sqrt{s_{NN}} = 200$ GeV for $0 < y < 0.8$, with brackets representing the point-to-point systematic error. The centrality bins are 0–10% (most central), 10–30%, 30–60%, and 60–100%. The lines are fits to the model predictions within the PHOBOS acceptance. The statistical error on the models is less than 2%. Figure taken from Ref. [16].

model curves, was that changing the centrality in d+Au collisions changes the ratio of transported protons to produced proton-antiproton pairs at a fixed pseudorapidity.

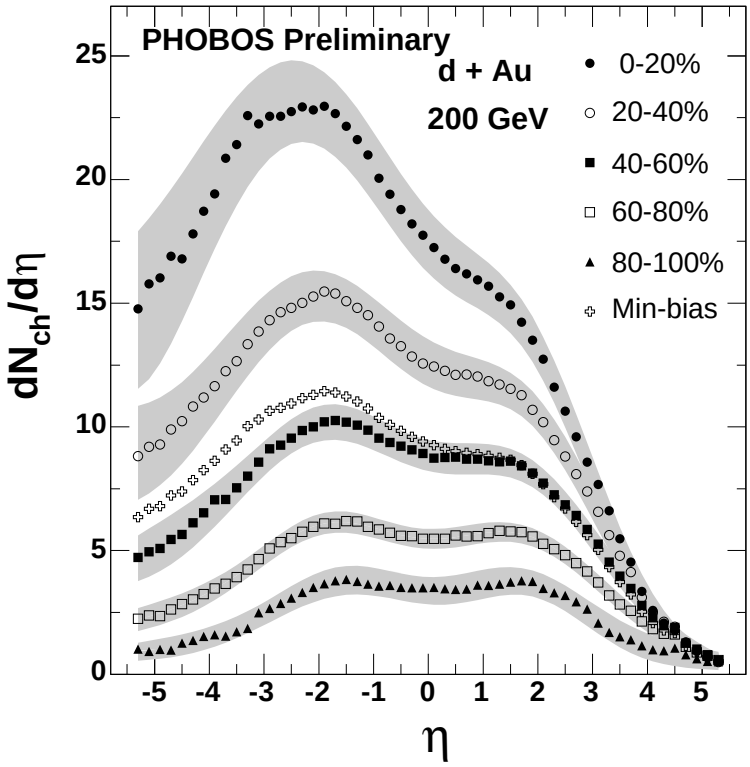

Figure 3. Centrality dependence of $dN_{ch}/d\eta$ distributions for $\sqrt{s_{NN}}$ = 200 GeV d+Au collisions for five centrality bins (0–20%, 20–40%, 40–60%, 60–80%, 80–100%). Shaded bands represent the systematic errors (90% C.L.). The minimum bias distribution [17] is shown as open diamonds. The centrality dependent data are preliminary. Figure taken from Ref. [32].

Figure 3 shows the preliminary pseudorapidity distribution for d+Au collisions as a function of centrality. These d+Au analyses required significant extensions to the vertex-finding and centrality-determination algorithms in order to handle very low multiplicity events efficiently. The centrality-determination algorithms take full advantage of the event-by-event determination of $dN_{ch}/d\eta$ which allows the use of integrated particle production in various regions of η to order the events in centrality. Because of this capability, the PHOBOS detector is probably the best-suited of all of the RHIC detectors to measure centrality in Si+Si events.

1.2. First Results from Run IV

The PHOBOS collaboration has already submitted two publications from Run IV: one on spectra (R_{AA}) [19] and one on elliptic flow [22]. These results extend the list of striking

empirical scaling phenomena seen so far by PHOBOS [33–35]. The new phenomena are "factorization" in the energy and centrality dependence of R_{AA} and "extensive longitudinal scaling" (limiting fragmentation) of elliptic flow in, effectively, the beam or target rest frame: $v_2(\eta')$.

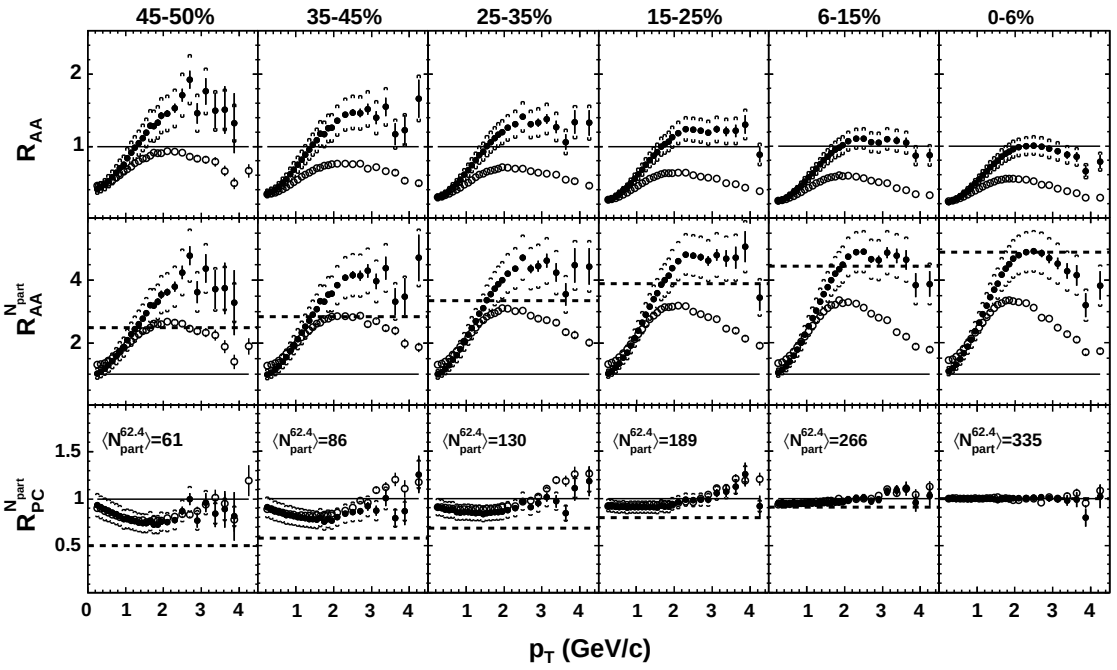

Figure 4. Ratio of p_T distributions from Au+Au collisions to various reference distributions at $\sqrt{s_{NN}} = 62.4$ GeV (filled symbols) and 200 GeV (open symbols). Data are shown in six bins of centrality, ranging from $\langle N_{part}\rangle = 61$ to 335 for 62.4 GeV collisions. The top row shows the nuclear modification factor R_{AA}, i.e. the ratio relative to proton-(anti)proton collisions scaled by $\langle N_{coll}\rangle$. The middle row shows $R_{AA}^{N_{part}}$, which uses proton-(anti)proton collisions scaled by $\langle N_{part}/2\rangle$. The bottom row shows $R_{PC}^{N_{part}}$, using a fit to central data scaled by $\langle N_{part}/2\rangle$ as a reference. The dashed lines in the middle and bottom rows indicate the expectation for N_{coll} scaling at $\sqrt{s_{NN}} = 62.4$ GeV relative to the reference distribution. Systematic uncertainties for all plots are shown by brackets (90% C.L.). Figure taken from Ref. [19].

Figure 4 shows the first result released from RHIC Run IV. The top row shows the conventional R_{AA} measurement for 62.4 and 200 GeV, showing the apparent interplay between a Cronin-like enhancement and hadron suppression at moderately high p_T. The middle row shows the same result, but normalized by $\langle N_{part}/2\rangle$. The residual centrality dependence is much weaker when normalized this way, suggesting that there is a geometric scaling according to $\langle N_{part}\rangle$ (or equivalently surface emission of high p_T hadrons) as we noted previously [33]. The new observation is that while both R_{AA} and $R_{AA}^{N_{part}}$ shows substantial energy and centrality dependences, when normalized by N_{part}, these depen-

dences seem to factorize. This can be seen in the bottom row of panels where the energy dependence for the central data has been explicitly factored out. A modest centrality dependence remains, and it is energy-independent for the region of $\langle N_{part} \rangle$ measured. It would be very interesting to see if such a factorization also occurs in a smaller system, such as Si+Si.

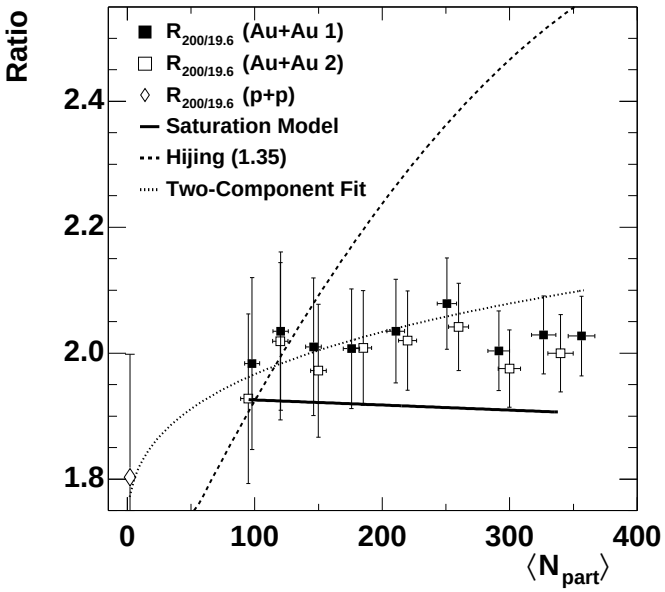

Figure 5. The ratio, $R_{200/19.6}$, of the midrapidity pseudorapidity density per participant pair at 200 and 19.6 GeV versus $\langle N_{part} \rangle$. The data binned by fraction of cross section are shown as closed squares and that binned by matching $\langle N_{part} \rangle$ are given as open squares. Also shown is the division of the inelastic p($\bar{\text{p}}$) + p collision data (open diamond) at $N_{part} = 2$. Curves give various calculations. The vertical error bars are combined statistical and systematic 1-σ uncertainties. Figure taken from Ref. [20].

This result is reminiscent of a precision measurement from Run II which is also among our recent publications [20]. Figure 5 shows the ratio of the scaled midrapidity pseudorapidity density at 200 and 19.6 GeV as a function of $\langle N_{part} \rangle$. Again we see a remarkable factorization between the centrality and energy dependences, indicated by the constant value of this ratio. The slope of the scaled pseudorapidity distribution was widely expected to change substantially from 19.6 to 200 GeV as the minijet cross-section increased. The HIJING curve in Figure 5 shows a typical example of this expectation.

Another new phenomenon which was observed in Run IV was the behavior of elliptic flow when viewed, effectively, in the rest frame of one of the colliding Au beams: $v_2(\eta')$. Figure 6 shows the elliptic flow for four different beam energies and the agreement over an extensive range of η' is remarkable. This result and the similar scaling in $dN/d\eta'$ reported previously [34], which we call "extensive longitudinal scaling" as they represent

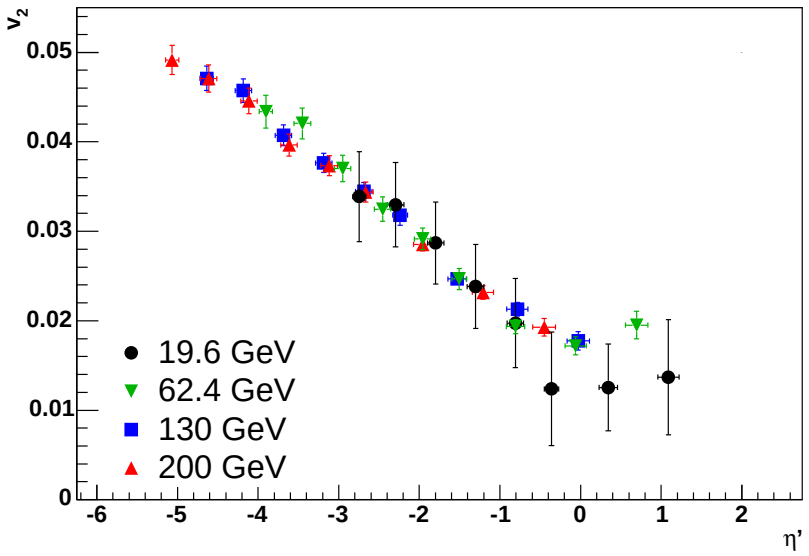

Figure 6. Elliptic flow, averaged over centrality (0-40%), as a function of $\eta' = |\eta| - y_{beam}$ for four beam energies. Systematic errors are not shown. Figure taken from Ref. [22].

a "limiting fragmentation" phenomenon [36] extended well past the region of expected validity. It is difficult to reconcile this result with the common assumption that the mechanism of particle production at midrapidity differs from that in the fragmentation region, particularly at the higher energies. They imply that the longitudinal degrees of freedom are not to be treated trivially in our experimental and theoretical efforts to understand these collisions.

Taken together, these empirical observations serve, at least, to characterize heavy ion collisions in an economical way and to challenge models. At best, the observed scaling and universalities may point the way to a simpler description of this high density matter and thus advance our knowledge of the strong interaction.

It should be noted that all of these results benefited greatly from the excellent Run IV statistics for 62.4 GeV Au+Au as well as the large difference in energies between 62.4 and 200 GeV.

1.3. Progress on the July 2003 Beam Use Proposal

Table 1 contains the original beam use request from last year along with the status of the various requests. The full energy and "63 GeV" Au+Au run requests were satisfied by the Au+Au running in Run IV. A major change from last year is that we are satisfied with our current 200 GeV p+p sample even though we did not reach our goal of a billion events. This change is based on new information which changes the cost/benefit ratio of taking a large data sample. On the "cost" side, it has become clear that it is a challenge for the machine to run p+p with more than two interaction regions leading to potential scheduling confusion and operating inefficiencies which negatively impact PHOBOS (and RHIC). On the "benefit" side, the mysterious difference in R_{dAu} between PHOBOS and the

other experiments has been confirmed to be due to a genuine pseudorapidity dependence and not a problem with the p+p reference data (see Figure 1). This lowers the priority of taking a high statistics p+p reference dataset.

Run Mode	Delivered $\int Ldt$	Events on Tape	Status
	Run IV 27–37 weeks		
Au+Au 200 GeV	33–260 $(\mu b)^{-1}$	110–640 M	COMPLETED
Fe+Fe 200 GeV	42–210 $(\mu b)^{-1}$	50–190 M	
	Run V 27–37 weeks		
p+p 200 GeV	1–3 $(pb)^{-1}$	840-1400 M	SUFFICIENT
Au+Au 63 GeV	2.3–12 $(\mu b)^{-1}$	6–45 M	COMPLETED
	Run VI 27–37 weeks		
p+p 500 GeV	1.4-1.8 $(pb)^{-1}$	480 M	
Further Energy/Species			

Table 1
Proposed running schedule from the July 2003 PHOBOS Beam Use Proposal and the status of the various requests.

The remaining items from last year are a light ion run (specified as Fe+Fe 200 GeV last year), a short run of high energy p+p, and the item called "Further Energy/Species". Below we will flesh out the "Further Energy/Species" request and reprioritize the remaining items based on the information gleaned from the last run.

2. Current Physics Priorities

Our highest priority has shifted from an intermediate mass ion run (Fe+Fe or Cu+Cu) to a light ion run (Si+Si). There are two motivations for this change. First, we want to start with an ion that is as different as possible from Au+Au while still providing an overlapping region of N_{part} between central AA and peripheral Au+Au. Si+Si provides this contrast. Second, the world data set on symmetric light ion collisions (Si+Si, Si+Al, S+S) [3–15] will allow us to put this data in better context.

Figure 7 illustrates both of these points. Not only do they show Si+Si and S+S data, but they also indicate that a Si+Si collision is different than a peripheral Pb+Pb collision at the same $\langle N_{part} \rangle$. In particular, the data in the leftmost set of panels shows that the strangeness "enhancement" seen in Si+Si is larger than that in peripheral Pb+Pb. In the middle set of panels, where the data are plotted versus the fraction of multiply struck partons, note that the Si+Si data, despite being at lower $\langle N_{part} \rangle$, is comparable to the mid-central Pb+Pb both in terms of the fraction of multiple collisions and the K/π ratio. The NA49 data indicates that this difference is at least important in strangeness production and may be important in other variables as well. Furthermore, we would be able to compare our results to that at lower energies much more cleanly if we use a similar size ion.

An intermediate mass ion run (now Cu+Cu) is now our second priority. It should be noted that we consider Cu, Ni and Fe to be functionally equivalent for our purposes. The

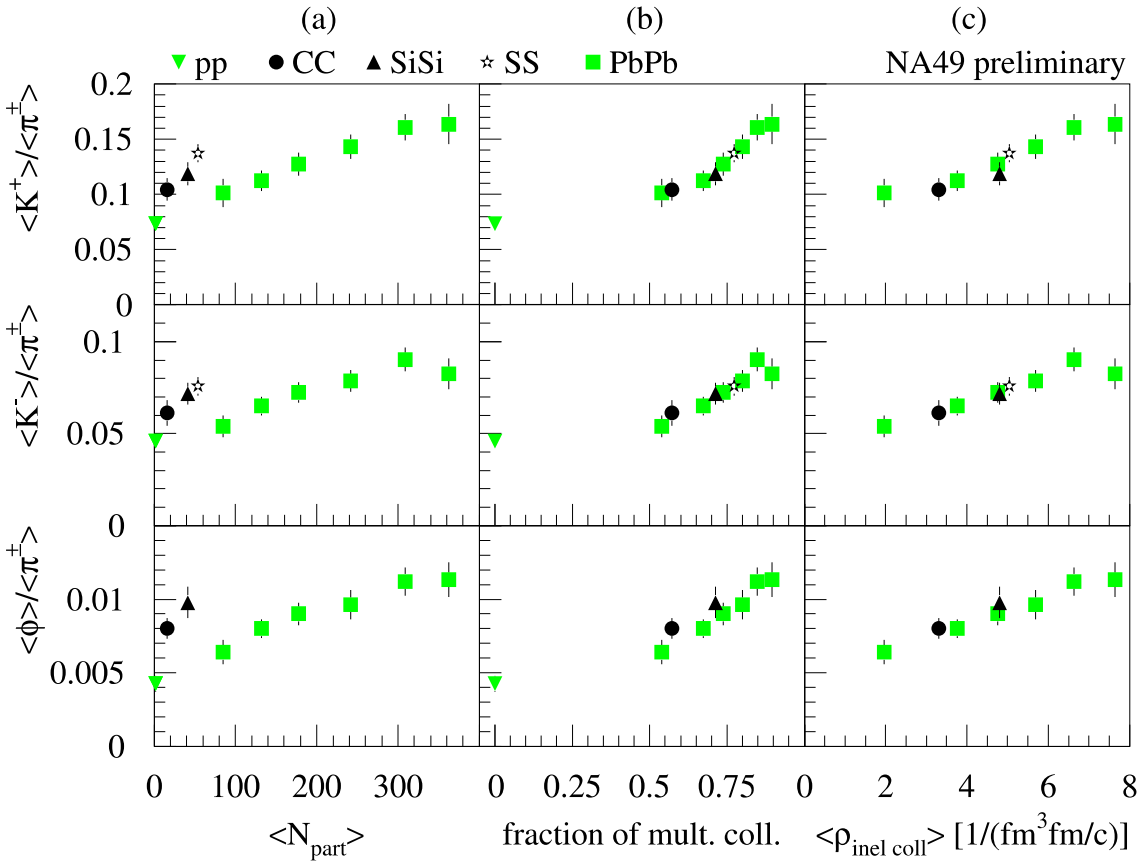

Figure 7. Strange particle to pion ratios from light ion collisions compared to p+p and Pb+Pb collisions at $\sqrt{s_{NN}} = 17.2$ GeV as a function of various centrality measures. The leftmost column uses the number of participating nucleons as a centrality measure. The middle column uses the fraction of multiply struck nucleons. The rightmost column uses the mean spacetime density of inelastic collisions when the nuclei first pass through each other in uRQMD. Figure taken from Ref. [14]. These data are preliminary.

choice between these should be made to optimize RHIC operations.

Based on the good experience in Run IV both with changing energies quickly and with high luminosity, we are requesting an energy scan for each of the light ion runs. Most of the running should still be at the highest energy, but a modest run at 62.4 GeV and a very short run at injection energy are also requested. The two highest energies would be used to study the interplay between the centrality and energy dependence of R_{AA} as discussed above for R_{AuAu} (see Figure 4) and for K/π ratios. All three energies would be used to measure $dN/d\eta$, $v_2(\eta)$ and $v_1(\eta)$ (see [37] for examples of v_1 measurements). PHOBOS has a unique (proven) capability to measure quantities such as $v_2(\eta')$ over 11 units of pseudorapidity. Once we are running a light ion species, we should fully exploit it by running three energies now as this measurement will be more difficult to make in the future.

The high energy p+p run request has been changed from 500 GeV to 400 GeV because we expect 400 GeV p+p collisions to match the effective energy of 200 GeV Au+Au collisions [35]. The key point here is that, again, there are some measurements that are unique to PHOBOS at high η and also at low p_T which will be lost if the high energy p+p engineering run is postponed until 2008 after the PHOBOS program is completed.

Finally we can imagine a suite of possible configurations that could be requested in Run VI after the results from Run IV and Run V are digested. These are generically labelled as "Further Energy/Species" and examples include, in no particular order, a longer 20 GeV Au+Au run, 200 GeV Si+Au, 200 GeV Au+d (deuteron beam in the yellow ring).

3. Proposed Running Schedule

In order to prepare the proposed running schedule, we followed the ground rules given in the June 26 version of the RHIC collider projections document [38]. Namely:

- 3 weeks for cryogenic cooldown and warm up
- 7 weeks total for setup and ramp-up for two beam species
- 0.5 weeks (2–3 days quoted) for each energy change.

If we run two species (Si+Si and p+p for instance) each at one energy, 10 weeks are spent in setup, leading to a total of 21 weeks of production physics running in a "31-week" run as outlined in the projections document. If we run two species (Si+Si and Cu+Cu for instance) with three energies each, this adds four energy changes and costs 2 weeks (conservatively), bringing the total production running down to 19 weeks.

In Table 2 we present the optimum schedule for extracting heavy ion physics results which are unique to PHOBOS as quickly as possible. This would involve an energy scan for symmetric collisions of both a light (Si) and intermediate (Cu) ion in FY05. In the 27 week scenario, we would give up the lower energy Cu+Cu running.

Since the Program Advisory Committee and lab management must balance many goals and pressures, we recognize that there may need to be a spin physics run in FY05. For this reason, in Table 3 we present the preferred schedule under the following constraints for run V:

Run Mode	Delivered $\int Ldt$ (31 wks. cryo.)	Running Time (31 wks. cryo.)	Fallback (27 wks. cryo.)
	Run V		
Si+Si 200 GeV	3.4–10 $(nb)^{-1}$	6 weeks	6 weeks
Si+Si 62.4 GeV	0.2–0.6 $(nb)^{-1}$	2.5 weeks	2.5 weeks
Si+Si 30 GeV	20–60 $(\mu b)^{-1}$	1 week	1 week
Cu+Cu 200 GeV	1–3 $(nb)^{-1}$	6 weeks	6.5 weeks
Cu+Cu 62.4 GeV	50–150 $(\mu b)^{-1}$	2.5 weeks	0
Cu+Cu 30 GeV	5–15 $(\mu b)^{-1}$	1 week	0
	Run VI		
p+p 400 GeV	1.4–1.8 $(pb)^{-1}$	4 weeks	4 weeks
Further Energy/Species			

Table 2
Proposed running schedule for Runs V and VI assuming 27 or 31 weeks of running and no requirement to run p+p at 200 GeV.

- Seven out of the twenty-one weeks (1/3) of expected production physics running is allocated to p+p spin physics.
- Only one light ion species is allowed.
- It is possible to deliver 200+200 GeV (or 250+250) GeV p+p test/engineering data for half a week after a one week setup.

If we run two species (Si+Si and p+p for instance) each at one energy, 10 weeks are spent in setup, leading to a total of 21 weeks of production physics running in a "31-week" run as outlined in the projections document. If we run two species (Si+Si and Cu+Cu for instance) with three energies each, this adds four energy changes and costs 2 weeks (conservatively), bringing the total production running down to 19 weeks.

In this case, we still propose an energy scan in Si+Si in Run V and we postpone the Cu+Cu energy scan until run VI. In this scenario, if it is feasible, we propose to take 1.5 weeks out of the light ion running to perform a 400 GeV p+p engineering/testdata run which would give enough data to measure $dN/d\eta$ and total N_{ch} for the higher energy p+p data in the same detector for comparison to 200 GeV Au+Au. As above, the total production running would be 19 weeks, with 7 devoted to p+p at 200 GeV, leaving 12 weeks for production running useful to PHOBOS. In the case of only 27 weeks of running (or 31 weeks of running with 11 weeks devoted to spin physics), we would postpone the 400 GeV p+p request until Run VI and reduce the Si+Si running slightly. This would leave 9 weeks of production running for PHOBOS.

Following two more runs of RHIC, we expect the baseline program of PHOBOS to be complete. Further run requests would only occur if a clear target of opportunity presents itself where the particular strengths of PHOBOS are needed for a particular measurement.

Run Mode	Delivered $\int Ldt$ (31 wks. cryo.)	Running Time (31 wks. cryo.)	Fallback (27 wks. cryo.)
	Run V		
Si+Si 200 GeV	5–16 $(nb)^{-1}$	8 weeks	6 weeks
Si+Si 62.4 GeV	0.2–0.6 $(nb)^{-1}$	2.5 weeks	2 weeks
Si+Si 30 GeV	20–60 $(\mu b)^{-1}$	1 week	1 week
p+p 200 GeV	N/A	N/A	N/A
p+p 400 GeV		0.5 weeks	0
	Run VI		
Cu+Cu 200 GeV	1.5–4.5 $(nb)^{-1}$	8 weeks	8 weeks
Cu+Cu 62.4 GeV	50–150 $(\mu b)^{-1}$	2.5 weeks	2.5 weeks
Cu+Cu 30 GeV	5–15 $(\mu b)^{-1}$	1 week	1 week
p+p 400 GeV	—	0	0.5 weeks
Further Energy/Species			

Table 3
Proposed running schedule for Runs V and VI assuming 27 or 31 weeks of running with 7 weeks of spin physics.

4. Summary

The PHOBOS detector provides unique capabilities at RHIC with a demonstrated ability to measure total charge multiplicity, $dN/d\eta$, and elliptic and directed flow over eleven units of pseudorapidity as well as spectra down to transverse momenta of 0.03 GeV/c. Additionally, the detector provides the ability to make reasonable centrality bins in small systems (such as d+Au or Si+Si) while minimizing biases.

We propose that the coming runs at RHIC be dedicated to providing as broad a variety of collision species and energies as possible in order to exploit the unique features of PHOBOS in a timely fashion before the experiment ends and these capabilities are lost, or at least diminished, at RHIC. In particular, we consider a light ion species, such as Si+Si, the highest priority because it enables the largest contrast with Au+Au while still showing differences from p+p [14]. Furthermore, lower energy Si+Si, Si+Al and S+S collision data exists to help contextualize any new results [3–15].

REFERENCES

1. Details can be found in the "white papers" of the four RHIC experiments currently in preparation.
2. J. Sandweiss *et al.* Report of the Brookhaven AGS-RHIC Program Advisory Committee, Dec. 2003.
3. G. Charlton *et al.*, Phys. Rev. Lett. **30** (1973) 574.
4. J. Bächler *et al.*, Phys. Rev. Lett. **72** (1979) 239.
5. Y. Eisenberg *et al.*, Nucl. Phys. **B154** (1979) 239.
6. T. Abbot *et al.*, Phys. Lett. **B271** (1991) 447.
7. J. Bächler *et al.*, Z. Phys. **C51** (1991) 97.
8. J. Bächler *et al.*, Z. Phys. **C52** (1991) 239.

9. T. Abbot *et al.*, Phys. Rev. Lett. **69** (1992) 1030.
10. T. Abbot *et al.*, Phys. Lett. **B291** (1992) 341.
11. T. Abbot *et al.*, Phys. Rev. Lett. **70** (1993) 1393.
12. J. Bächler *et al.*, Z. Phys. **C64** (1994) 195.
13. T. Abbot *et al.*, Phys. Rev. **C50** (1994) 1024.
14. C. Höhne *et al.*, Nucl. Phys. **A715** (2003) 474c.
15. I. Krauss *et al.*, J. Phys. **G30** (2004) S583.
16. B.B. Back *et al.*, Phys. Rev. **C70** (2004) 011901(R).
17. B.B. Back *et al.*, Phys. Rev. Lett. (2004) in press, arXiv:nucl-ex/0311009.
18. B.B. Back *et al.*, submitted to Phys. Rev. Lett., arXiv:nucl-ex/0401006.
19. B.B. Back *et al.*, submitted to Phys. Rev. Lett., arXiv:nucl-ex/0405003.
20. B.B. Back *et al.*, Phys. Rev. C(RC) in press, arXiv:nucl-ex/0405027.
21. B.B. Back *et al.*, submitted to Phys. Rev. C(RC), arXiv:nucl-ex/0406017.
22. B.B. Back *et al.*, submitted to Phys. Rev. Lett., arXiv:nucl-ex/0406021.
23. B.B. Back *et al.*, submitted to Phys. Rev. C(RC), arXiv:nucl-ex/0407012.
24. B.B. Back *et al.*, Phys. Rev. Lett. **91** (2003) 072302.
25. S.S. Adler *et al.*, Phys. Rev. Lett. **91** (2003) 072303.
26. J. Adams *et al.*, Phys. Rev. Lett. **91** (2003) 072304.
27. I. Arsene *et al.*, Phys. Rev. Lett. **91** (2003) 072305.
28. I. Arsene *et al.*, submitted to Phys. Rev. Lett., arXiv:nucl-ex/0403005
29. M.X. Liu *et al.*, arXiv:nucl-ex/0403047.
30. D. Kharzeev,Y.V. Kovchegov, and K. Tuchin, arXiv:hep-ph/0405045.
31. A. Accardi, arXiv:nucl-th/0405046.
32. R. Nouicer *et al.*, arXiv:nucl-ex/0403033.
33. B.B. Back *et al.*, Phys. Lett. **B 578** (2004) 297.
34. B.B. Back *et al.*, Phys. Rev. Lett. **91** (2003) 052303.
35. B.B. Back *et al.*, submitted to Phys. Rev. Lett., arXiv:nucl-ex/0301017.
36. J. Benecke, T.T. Chou, C-N. Yang, E. Yen, Phys. Rev. **188** (1969) 2159.
37. M.B. Tonjes *et al.*, arXiv:nucl-ex/0403025.
38. T. Roser, W. Fischer, M. Bai, F. Pilat, "RHIC Collider Projections (FY2005-2008)", (July 26, 2004).